5-2014

Methods to Enhance Spent Fuel Pool and Dry Cask Storage

Dustin Giltnane
University of Tennessee - Knoxville, dgiltnan@vols.utk.edu

David Gotthold
University of Tennessee - Knoxville, dgotthol@vols.utk.edu

Seth Langford
University of Tennessee - Knoxville, slangfo1@vols.utk.edu

Michael Ratliff
University of Tennessee - Knoxville, mratlif6@vols.utk.edu

Jessica Dawn Shewmaker
University of Tennessee - Knoxville, jshewma1@vols.utk.edu

See next page for additional authors

Methods to Enhance Spent Fuel Pool and Dry Cask Storage

Dustin Giltnane

Dave Gotthold

Seth Langford

Michael Ratliff

Jessica Shewmaker

Cody Wiggins

Professor: M. L. Grossbeck, Ph.D.

Abstract

This report presents two solutions. One to extend the time of spent fuel pool coolant boil off during station black out conditions and the other to diminish criticality during long-term, dry cask storage of spent fuel. The molten salt Hitec was found to be not only a viable option as spent fuel pool coolant, but it will also provide the necessary time for decay heat removal without the danger of boil-off or the possibility of degradation due to radiation exposure. Additionally the project examines the possibility of dipping commercial zircaloy fuel rods in an alloy solution before movement to dry storage providing a coating which would add a neutron poison to the outside of the zircaloy fuel rod. Experiments showed that 60Zn-40Cd alloy is capable of wetting to zirconium and provides a substantial neutron poison while not contributing to an increase in peak cladding temperatures. A SCALE model verified the ability of this alloy to maintain criticality control in current SFP and dry cask conditions, as well as in the postulated Hitec spent fuel pool. Heat transfer in dry cask conditions was modeled using COMSOL. Alloy coated rods were modeled first using normal spacing and then a reduced spacing for the fuel rods. The simulation showed no significant increase in peak cladding temperature for normal spacing but a slight increase in temperature for the compacted array, indicating that a larger scale model may be necessary to ensure dry cask safety in the case of increased fuel density.

Acknowledgements

The authors would like to express their sincerest thanks to all who have assisted in the formulation and implementation of this project. First, we thank Dr. Martin L. Grossbeck for his leadership and guidance during this endeavor. We also thank Dr. Arthur E. Ruggles for his assistance in our thermal analyses and Gregory Jones for his assistance in the use of the scanning electron microscope. Lastly, we thank the Electric Power Research Institute for its financial assistance for this project.

Table of Contents

List of Figures

List of Tables

Purpose and Background

Following the Fukushima Daiichi accident, the prevention of coolant boil-off in the spent fuel pool (SFP) arose as an issue to be addressed by the nuclear community. On March 11, 2011 the Fukushima Daiichi Nuclear Power Station was hit by a magnitude 9.0 earthquake off the coast of Honshu, Japan which caused a SCRAM of the three operating nuclear reactors. The earthquake caused the site to lose all offsite electrical power. As designed, the emergency diesel generators were automatically started, providing power to the site and allowed emergency cooling of the reactors and spent fuel pool. Normally this backup system would be used until offsite power was restored and the reactors resume routine operation, however, shortly after the earthquake struck the power plant was the victim of a tsunami, which was estimated to be around 60 feet high. The emergency diesel generators were located below ground level and were flooded, causing them to fail. At this point, the three reactors as well as the spent fuel pools ceased forced cooling. Thus began a series of events whose consequences have greatly impacted the nuclear industry. Since cooling was removed from the reactors and fuel, fission product decay resulted in the continuous heating of the fuel elements. Over the course of a day it was ascertained that the core fuel elements in the reactors were uncovered and the fuel had started to melt. On March 12, a hydrogen explosion occurred, damaging the reactor building of the unit 1 reactor and exposing its SFP to the atmosphere. Two days later, a second hydrogen explosion occurred in reactor 3, causing the containment unit to be damaged and exposing the spent fuel pool to atmosphere. It was determined at this time that all three reactors had water levels below the fuel elements and that all three reactors were experiencing fuel damage. On March 15, two more hydrogen explosions occurred, one in unit 2 containment and one in unit 4 containment. At this time the unit 4 SFP fuel was feared to be uncovered due to boiling. In reality, the fuel in the affected SFP was not fully uncovered. However, the event and concern that surrounded it proved new methods for preventing coolant boil-off would be advantageous for the nuclear industry to consider. Additionally, the lack of major long-term storage for used nuclear fuel has created an issue with SFP and dry cask storage overcrowding. For this reason, an increase in dry cask fuel density would be advantageous for the interim storage of used fuel, but criticality control must be maintained in such a compacted fuel scenario. In order to address these concerns, this

investigation considers a replacement coolant in the SFP and explores adding a neutron poison coating to the spent fuel rods after leaving the SFP in hopes of more densely packing the rods in dry storage while maintaining safety.

After a fuel rod has been removed from a reactor core, the heat generated due to continued radioactive decay is dangerously high. This decay heat creates a problem for storage due to the degradation of the fuel cladding. The reliability of this system is of paramount importance in preventing the release of radiation to the public. Currently, pure water pools are used for storage of these rods until the decay heat has decreased sufficiently for the fuel to be placed in dry cask storage. The current method of dry cask storage is to place the fuel rods in an egg crate lattice structure within a containment vessel, or cask, which holds them indefinitely with the ultimate goal of placing them into a repository at a later date.

The SFP is either connected to or in close proximity to the reactor containment of a commercial power plant.[1] When a reactor has adequately used the U-235 fuel, its bundles must be extracted from the core. Depending on whether the system is a pressurized water reactor (PWR) or boiling water reactor (BWR) this extraction method varies slightly. For PWRs the fuel bundle is passed through a transfer tub to the spent fuel storage facility, as shown in Figure 1.

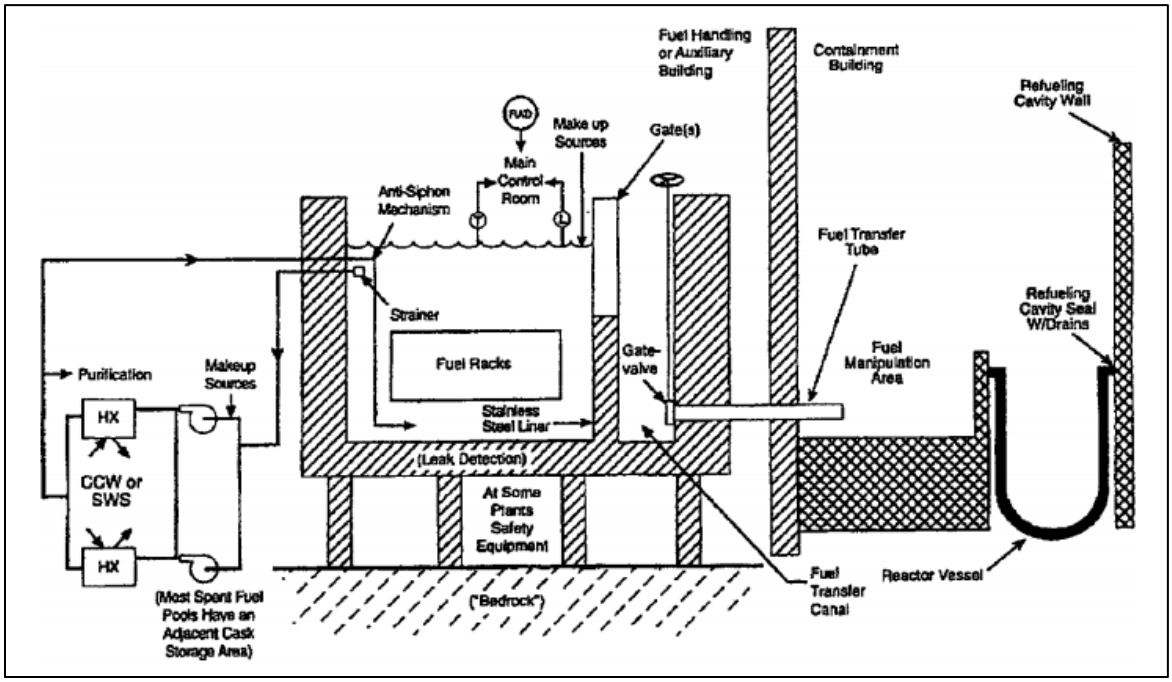

Figure 1 Layout of a spent fuel pool and associated transfer system for a PWR (Source: NUREG-1275, 1997)[2]

After being relocated, the fuel bundle resides in the SFP for approximately five years before being transferred to onsite dry cask storage. BWRs, however, utilize a system in which the reactor compartment is flooded, as shown in Figure 2.

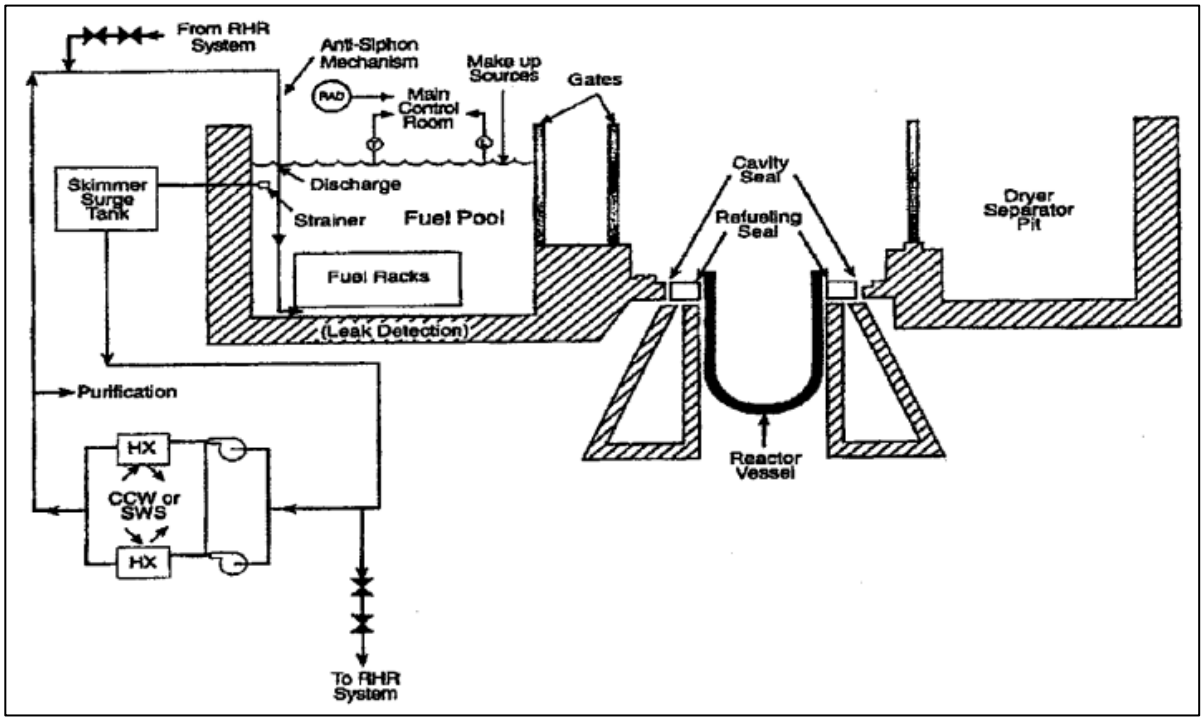

Figure 2 Layout of a spent fuel pool and associated transfer system for a BWR (Source: NUREG-1275, 1997)[2]

After flooding and exposing the core, the fuel bundle is removed. The bundle travels through two sequential gates before arriving at the SFP. The bundle is placed in the fuel rack, and the reactor compartment is drained down to normal levels. As in the PWR case, the fuel bundle will sit in the SFP for several years before being placed in onsite dry cask storage.

The industry already has several methods for elongating time to boil in the SFP as well as decreasing the neutron population. Current designs regulate neutron population by using Boral, a neutron poison, in the SFP. Boral consists of a boron carbide chemical contained in an Aluminum 1100 alloy "plate" which is placed around the perimeter and between the individual bundles for criticality safety concerns. Boral decreases the criticality of the pool by acting as a poison when fuel bundles have to be placed closer together to maximize space for more spent fuel. Previously Boraflex, a boron carbide in a matrix of polydimethyl siloxane or silicone rubber, was used as a neutron poison in the SFP. However, Boraflex deteriorated when exposed

to gamma radiation generated from the spent fuel bundles for an extended time period, making the SFP less safe. Due to this unfortunate reaction Boraflex is no longer utilized.

Due to the dangerous materials produced from nuclear fission, it is imperative to ensure proper conditions are maintained pertaining to water chemistry. Table 1, below, provides a brief overview of the recommended water conditions as per the IAEA suggestions.

Good Practices for Water Quality Management in Research Reactors and Spent Fuel Storage Facilities, IAEA	
pH	4.5-7
Cooling water	Demineralized Water
Conductivity	<10µS/cm
Copper	<.1mg/L
Chlorides	<.1mg/L
Sulfate	<10mg/L
Nitrate	<10mg/L
Solids	<1mg/L
Iron	<1.0mg/L
Aluminum	<1.0mg/L
Temperature	<45 deg C
Cs137	.02MBq/m2
Water Activity	20MBq/m2

Table 1 Suggested Spent Fuel Pool conditions as per IAEA standards

Water quality is a concern when dealing with nuclear fuel since corrosion of the fuel cladding is detrimental to the defense in depth policy. Through the course of the fuel's life in an operating nuclear reactor, the fission of U-235 results in the formation of radioactive daughter particles. These fission products decay and continuously release heat which must be removed. Another issue associated with the radioactive decay is production of daughter radioactive gasses. These gasses are contained inside the fuel and cladding and therefore are no harm to those working around the fuel. However, if the cladding or fuel were to crack, these gases could then escape

into the atmosphere. Because of this, concern for fuel integrity arises. These gases can be inhaled unknowingly and decay inside the body. Since most of these fission products decay via alpha particle emission, this decay process poses great health risks to any biological entity within proximity to the fuel. While alpha particles are of little concern outside the body, if emitted from inside a person's body, the particle will readily interact with the electrons of surrounding atoms and thus damage cell DNA either directly or indirectly via formation of hydroxyl and hydronium molecules. The formation of CRUD is another cause for concern stemming from corrosion. CRUD is defined as the particles that fall from the main structures as a result of corrosion. An example of this is the dusting that forms underneath a car as it rusts. This dusting, while harmless from steel, is dangerous when dealing with nuclear materials due to their radioactivity. Once again this process poses the same issue as above. While there are methods implemented to remove CRUD from a system, the formation of CRUD is undesirable due to the fact that unforeseen radioactive hotspots can occur where none were thought to exist. CRUD can also pose risks when transferring the fuel bundles from wet to dry storage.

The modern dry cask storage container consists of an egg crate lattice structure that holds the fuel bundles. Immediately around the outside of the cask is a neutron absorbing material surrounded by a gamma shielding material. The gamma shielding material, typically a part of the metal cask, is placed outside the neutron absorbing material due to secondary gammas that are released from neutron interactions. The cask is constructed inside the plant and then placed into the SFP where the fuel bundles are transferred into it. The entire process must remain underwater to minimize exposure to workers and to maintain cooling of the fuel bundles. After all bundles have been transferred, the cask is removed from the SFP and rinsed to remove any contamination that remains on the outside of the cask. The water within the cask is then replaced with helium. Once the fuel bundles have been sealed and all necessary precautions have been taken, the cask is transferred to an onsite holding area. The cask is stored on site until it is transferred to a permanent storage facility.

Proposed Solution for the Spent Fuel Pool

The group was tasked with creating a way to extend the time of spent fuel pool coolant-boil off during station black out (SBO) conditions. During SBO conditions one must assume that active cooling mechanisms inside of the spent fuel pool no longer work. This assumption means the pool inventory's temperature will increase as decay heat from the used nuclear fuel deposits heat into the pool. Eventually the pool will begin to boil unless some form of active cooling takes place. To increase the amount of time it takes for the SFP to reach boiling temperature and improve safety, the group decided to replace the water inside of the SFP with a different liquid that would perform better than water under SBO conditions.

One of the major difficulties with the investigation was finding a fluid that had thermophysical properties more favorable than water. One of the reasons why water is so hard to replace is that is has an exceptional heat capacity of around 4.18 $\frac{kJ}{kg-^{\circ}C}$ (C_p), a density of around 1000 $\frac{Kg}{m^3}$ (ρ), and an emissivity (ϵ) near one. The major weakness of water is a relatively low boiling point of 100 °C, giving it a relatively small temperature difference (ΔT) between regular operating conditions and onset of boiling. To be a viable replacement for water the proposed liquid would require a $\rho C_p \Delta T$ term competitive with water. The investigation did not find a chemical additive that would be accepted by current nuclear power plants (NPP) and would both withstand the extreme conditions associated with close proximity to the fuel and adequately increase the time it would take to reach the boiling point. The focus quickly switched to low-temperature molten salts due to their comparatively high density and a very large ΔT term needed to overcome the large heat capacity of water. While this radical change in coolant would not be possible for current NPP, future plants could implement such a design to increase safety of the SFP. After much searching, the leading candidate is a salt made by the Coastal Chemical Company called Hitec. To be a good molten salt for the SPF, the salt must have a sufficiently low melting temperature yet still provide a large ΔT term. In addition, the salt must also not release toxic fumes nor should it degrade or react violently with the fuel rods or any structural material with which it comes into contact.

Hitec Molten Salt

Hitec is the proposed molten salt to be used as a coolant in the SFP. Table 2, below, shows a comparison important thermophysical properties of water and Hitec at their liquid temperatures of 30°C and 142 °C, respectively. The lower heat capacity of the Hitec salt is overcome by its high density and very large ΔT value. Hitec's very large $\rho C_p \Delta T$ term shows that it can absorb nearly four times as much energy as water per unit volume before it reaches its maximum operating temperature.

	Water	**Hitec**
Density $\frac{kg}{m^3}$	995	1979
$\boldsymbol{Heat\ Capicty\ \frac{kJ}{kg-C}}$	4.18	1.56
ΔT from operational to maximum operating Temperature °C	70	396
Emissivity	.96	~.3
$\boldsymbol{\rho C_p \Delta T\ \frac{kJ}{m^3}}$	2.9*10^5	1.2*10^6
Melting Point °C	0	142
Boiling/Decomposition Point °C	100	~800
Maximum Rated operating Temperature °C	<100	538
Composition by Mass	11% H 89% O	7% NaNO3 50% KNO3 40% NaNO2

Table 2 Comparison of the thermophysical properties of water and Hitec salt

Two of the of the advantages of the Hitec salt are its relatively low melting point at 142 °C and large maximum operating temperature of 538 °C. Hitec has proven to not be detonable at

operating and melting temperatures. Also, it does not release toxic vapors when it is heated. However, ventilation should be supplied in the event that contaminants fall into the salt and release toxic fumes. While liquid, Hitec is a transparent yellow color which is beneficial because no special equipment or instrumentation will be needed to view the used fuel bundles.[6] If water were to come into contact with Hitec, its significantly lower density would allow the water to float on top of the pool while the salt would stay unaffected below. Lastly, Hitec salt has a relatively low cost of approximately $1/kg.

When dealing with a molten salt such as Hitec certain precautions must be taken into account for the design of the SFP as far as what materials can be used. Hitec salt should be kept away from combustible materials due to its high temperature. Hitec should not be ingested because it contains sodium nitrate, which is lethal if ingested. While the salt itself is not itself combustible, special care should be taken to keep it away from wood, magnesium, coke, plastic, cyanides, chlorates, ammonium salts, and active metals[6]. Magnesium and aluminum should be avoided unless special precautions are taken. In addition, iron should also be kept away from Hitec due to the possibility of an exothermic reaction. Table 3, below, shows ORNL's qualitative analysis of Hitec's corrosive properties on steel alloys over time. To mitigate corrosion and potential reactions with Hitec, stainless steel should be used as the main structural material.[6]

Alloy	Time yr.	Temp. °F	Blanket Gas	System	Comment
	3	800	Air	Circulating	No noticeable corrosion
ASTM-A-285 Grade C Carbon Steel	3	785-800	Limited Air	Circulating	No noticeable corrosion
	2.5	875	Steam	Circulating	No noticeable corrosion
347 SS	1.3	1050	Air	Heat Treat Bath	Negligible corrosion
347 SS	2	1000	Steam	Circulating	No noticeable corrosion
Seamless Stainless Tubing	0.8	930-1020	?	Circulating	No visible attack

Table 3 ORNL qualitative analysis of corrosion caused by Hitec molten salt on steel alloys[6]

Additionally, experimentation from ORNL, shown in Table 4, indicates some quantitative corrosion about the Hitec molten salt on materials other than just steel.

CORROSION OF METALS BY "HITEC"

Metals	Corrosion Rate, Inches Penetration Per Month						
	612°F.	785°F.	850°F.	1000°F.	1058°F.		1100°F.
					1st Period	2nd Period	
Steel—open hearth (ASME # S-17)	—	—	0.0003	0.001 to 0.002	—	—	0.01 to 0.05
Alloy steels							
15-16% chromium iron	—	—	—	0.0000	—	—	—
"Alcrosil" # 3	—	—	0.0002	0.001	—	—	0.002 to 0.006
"Alcrosil" # 5	—	—	0.0002	0.0005	—	—	0.001 to 0.002
Stainless steels							
Type 304	—	—	—	0.0007	—	—	—
Type 304L	—	—	—	0.0006	—	—	—
Type 309 (annealed)	0.00002	0.00001	0.0000	—	0.00110	0.00064	—
Type 309 Cb	—	—	—	—	0.00156	0.00094	—
Type 310	—	—	—	—	0.00117	0.00077	—
Type 316	—	—	—	0.0000	—	—	—
Type 321	—	—	—	—	0.00111	0.00056	—
Type 347	—	—	—	0.0004	0.00109	0.00068	—
Type 446	—	—	—	—	0.00146	0.00072	—
Inconel	—	—	—	0.0000	0.00153	0.00151	—
Carpenter 20	—	—	—	—	0.00097	0.00059	—
"Hastelloy" B	0.00011	0.000003	—	—	—	—	—
Monel	—	—	—	0.0001	—	—	—
Bronze	0.00006	0.00008	0.0001	—	—	—	—
Phosphorized Admiralty	0.00006	0.00005	0.0001	—	—	—	—
Copper	—	—	—	0.03	—	—	—
Nickel	—	—	—	—	—	—	0.00025

Table 4 ORNL Quantitative corrosion analysis caused by Hitec molten salt[6]

As indicated in Tables 3 and 4, stainless steel 316, 446, alloy steels with 15% chromium ions, Hastelloy B, and nickel are all acceptable construction materials due to the slow corrosion rate. However, other materials can be used so long as they are designed to take into account the corrosion from the salt over the length of the materials' lifetime.

By using Hitec instead of water, the SFP will need to be designed differently to accommodate Hitec's characteristic properties. The higher density might need to be considered due to an overall increase in the weight of the SFP. Heaters will be needed in the pool to keep the temperature above Hitec's freezing temperature, 142 °C, to avoid damaging pumps and to ensure adequate flow. To keep the room habitable some form of cooling will be needed during operations due to the heat released from the salt. Also, the salt's melting point will increase when exposed to air due to the oxidization of nitrite in the salt. Possible solutions involve either

periodically replacing the old salt with new salt in the pool or using a blanket gas over the pool to prevent oxidation. Figure 3 shows the rate at which the melting point increases when the salt is kept at 593 °C (1100 ° F) over a set time period. If the salt is covered in air, then it will be necessary to replenish the salt often to ensure the melting point does not get too high. If the salt is to be covered with a blanket gas, then the recommended gas would be Nitrogen due to its cost and safety.

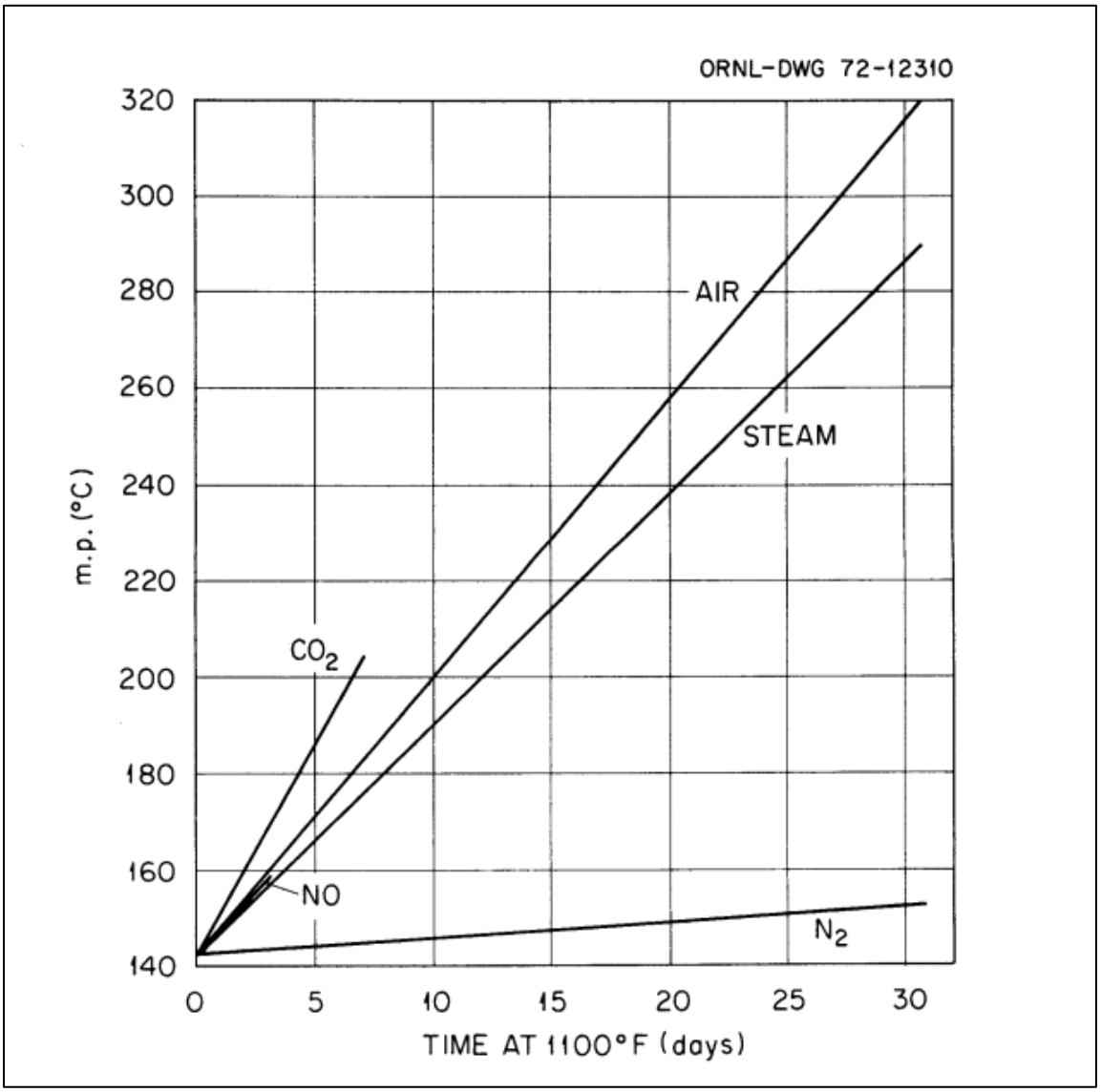

Figure 3 Cover Gases Effect on the Salts Melting Point[6]

Although there are many concerns with using Hitec as the coolant for the SFP there is compelling evidence which demonstrates the benefits outweigh the costs this new solution would bring.

Methodology for Pool Boil Calculations

A spent fuel pool heat up simulation was constructed using the information from NUREG-1353 section 4 regarding the dimensions of a typical spent fuel pool and spent fuel heat loads. The calculation used a stepping approach, in which the change in time, Δt, was calculated as the time in which the pool would heat up by a small amount, ΔT, according to the following equation:

$$\Delta t = \frac{(mC_p\Delta T)}{Q_{in} - Q_{out}} \qquad \text{Equation 1}$$

where m is the mass of the pool, C_p is the heat capacity, and Q_{in} and Q_{out} are the inflow and outflow of heat, respectively. After this the properties of the pool were updated to the next temperature, and the next time step was calculated. Beginning at regular operating conditions, this process continued until pool coolant failure, with the sum of all the calculated time steps being considered the total time to coolant failure.

Equations, which described the thermophysical properties of water and air as function of temperature, were taken from NIST and were used in the simulation. The equations, which governed the thermophysical behavior of Hitec, were found in an Oak Ridge National Laboratory report[6].

The method for calculating the amount of time it would take to raise the temperature by ΔT was calculated using an energy balance over the volume of the pool. As in the model described in NUREG-1353, the pool's volume was assumed to be 906 m^3 (32,000 ft^3), the pool is assumed to heat uniformly, and evaporative heat loss is neglected. In the model, heat is dissipated from the pool via natural convection into the air and walls and via radiation from the surface of the pool. Decay heat from the used fuel was taken to be the only heat source with heat generation strengths taken from load scenarios described in Table 4.6.3 from NUREG-1353. The decay heat values presented are based on that from the spent fuel of a 3000 MW thermal pressurized water

reactor. In all cases, a background decay heat value of 1.02 MW (3.5 million BTU/hr) is taken into account, simulating the accumulation of 20 years' worth of fuel at a rate of 1/3 core offload per year. The first scenario investigated assumes SBO after a 1/3 core offload. To maintain consistency with the NUREG-1353 model, for the water pool, the initial temperature is assumed to be 51.7 °C (125 °F). In the second scenario, time to pool boiling is investigated for SBO after a full-core offload. In this case, the initial pool temperature for water is assumed to be 65.6 °C (150 °F). For both cases, time to pool boil is calculated for a range of times after core offload. A third case investigates a worst-case scenario in which SBO occurs only 5 days after core offload. In this case, the initial water temperature is assumed to be 51.7 °C (125 °F), and time to boiling is calculated for a range of core offload sizes, from no core offload to full core offload. Each of these calculations was then repeated using Hitec as the pool coolant medium. In all Hitec cases, the initial temperature was taken to be 160 °C, and pool heating was tracked until the pool reached Hitec's maximum recommended operating temperature of 538 °C. The results seen below cite the calculated time to "coolant failure." In the case of water coolant failure is defined to be boiling (100 °C), whereas in the Hitec case, coolant failure is defined to be the maximum recommended operating temperature (538 °C).

Simulated Pool Boil Results

The calculated results for the amount of time it took to boil the pool when the cooling medium was water closely approximated the values listed in NUREG-1353, as seen in the Tables 5 and 6 below. With this validation of our calculation procedure, the calculated time to failure values for Hitec are considered fair approximations as well.

One-Third Core Discharge				
Days After Shutdown	Decay Heat (Watts)	**Water**		**Hitec**
		Heat up: 51.7 degC - 100 degC (hours)		Heat up: 160 degC - 538 degC (hours)
		Tabulated[7]	Calculated	Calculated
5	4.38E+06	11.2	11.5	68.9
10	3.54E+06	13.9	14.2	87.1
30	2.57E+06	19	19.7	125.2
45	2.25E+06	21.8	22.7	146.9
65	2.02E+06	24.3	25.3	167.6
100	1.78E+06	27.5	28.9	196.4
150	1.53E+06	32	33.9	240.9
200	1.40E+06	35.1	37.3	274.3
250	1.32E+06	37.2	39.6	299
300	1.27E+06	38.4	41.1	314.9
350	1.25E+06	39.2	42	325.4
365	1.24E+06	39.3	42.1	326.6

Table 5 Comparison of pool heat up times for water and Hitec for one-third core offload at various times after shutdown. All decay heat values include 1.02 MW from 20 years of build-up

Full Core Discharge				
Days After Shutdown	Decay Heat (Watts)	**Water**		**Hitec**
		Heat up: 65.6 degC - 100 degC (hours)		Heat up: 160 degC - 538 degC (hours)
		Tabulated	Calculated	Calculated
5	1.12E+07	3.1	3.2	25.9
10	8.65E+06	4.1	4.1	33.8
30	5.77E+06	6.1	6.2	51.8
45	4.78E+06	7.4	7.5	63.4
65	4.07E+06	8.6	8.8	75.4
100	3.37E+06	10.5	10.7	93
150	2.51E+06	13.6	14.5	130.2
200	2.19E+06	16.1	16.7	153.6
250	1.95E+06	18.1	18.9	177.1
300	1.82E+06	19.3	20.3	193.1
350	1.74E+06	20.2	21.3	205
365	1.73E+06	20.4	21.4	206.4

Table 6 Comparison of pool heat up times for water and Hitec for full core offload at various times after shutdown. All decay heat values include 1.02 MW from 20 years of build-up

Figures 4 and 5, below, show the trend in time-to-failure performance for both Hitec and water pools over various times after SBO. It can be clearly seen that in both the 1/3 and full core offload cases, the Hitec pool gives roughly 10 times the response time of the water pool

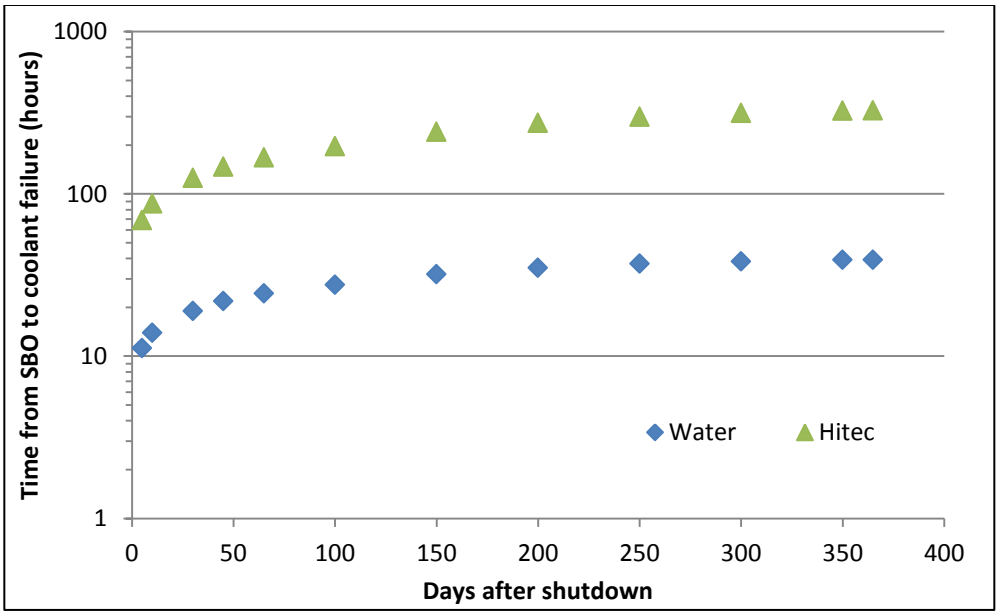

Figure 4 Comparison of pool heat up times for water and Hitec for one-third core offload at various times after shutdown.

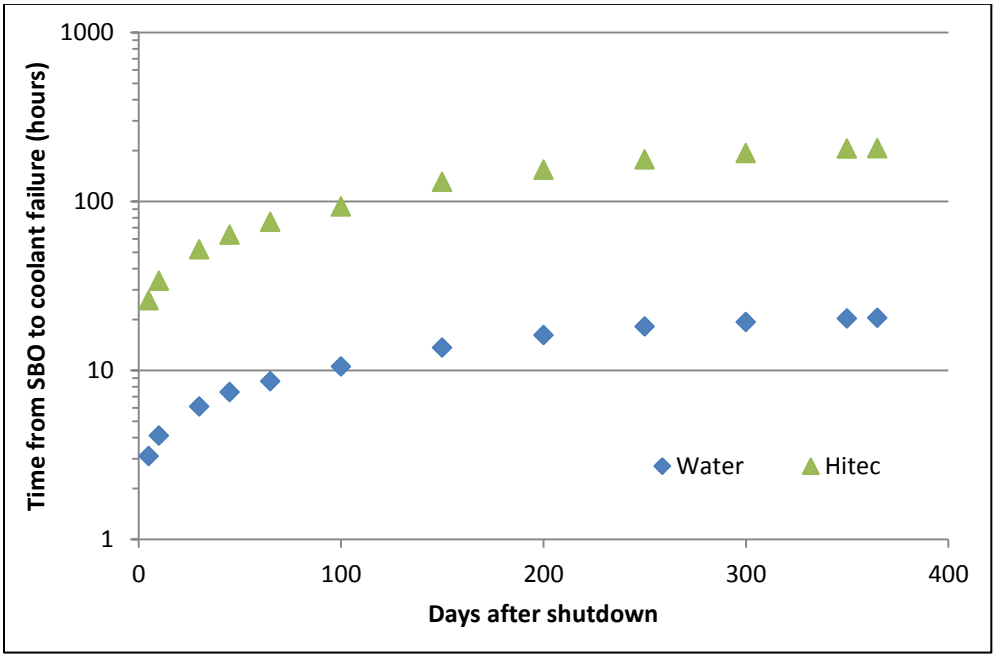

Figure 5 Comparison of pool heat up times for water and Hitec for full core offload at various times after shutdown.

Lastly, Figure 6 shows the trend in Hitec and water performances for varies amounts of core offload. Once again, there is a considerable increase in time-to-failure for the Hitec pool when compared to the water pool.

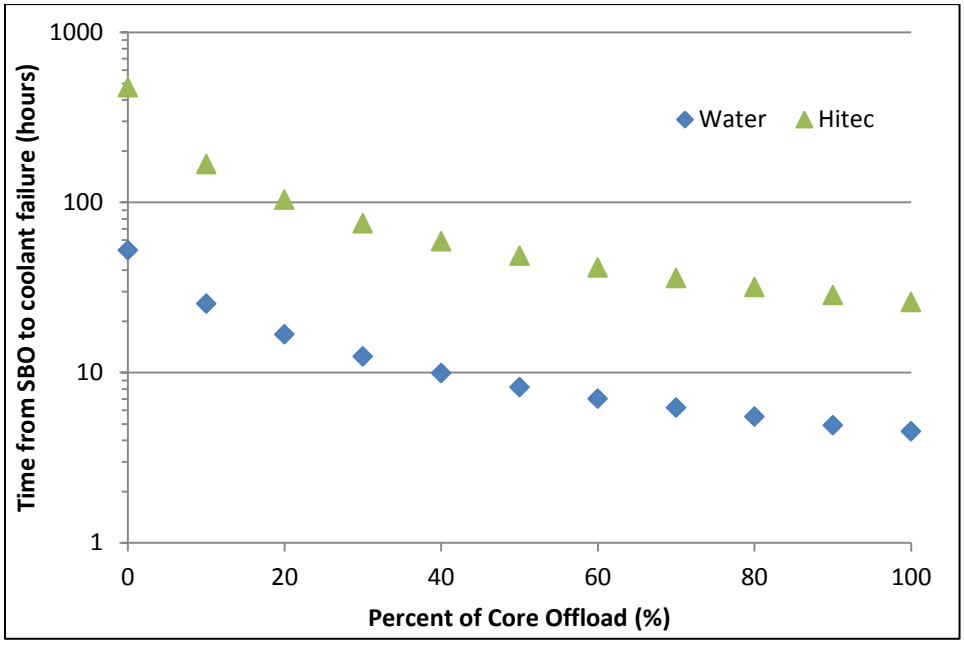

Figure 6 Comparison of pool heat up times for water and Hitec versus percent of core offload for SBO 5 days after shutdown. All offload is considered on top of decay heat from 20 years of build-up.

In terms of allowed response time after SBO, the Hitec pool's performance is far superior to the performance of water. Furthermore, it should be noted even though the maximum operational temperature of Hitec is at 538 °C, this is a conservatively recommended maximum temperature. The salt does not begin to undergo degradation until 800 °C. Thus it is likely that a Hitec pool could allow even more time until failure after SBO than the times given above.

Proposed Solution for Coating

The group also investigated the possibility of coating the spent fuel rods and/or bundles in a neutron poisoning material. The overarching goal is to increase storage density and safety for dry cask storage and other long-term applications. The basic concept involves adding an alloy coating during transition from wet pool storage to dry cask. The fuel rods would be lifted out of the pool and, if necessary, cleaned using a series of caustic and acidic solutions before being dipped in the molten alloy. It is probable that corrosion of the rod surface by the molten salt coolant in the fuel pool would provide the necessary caustic cleaning described above, but future experimentation is necessary to test this hypothesis. In the event that a cleaning dip is necessary, this process would happen between rod removal from the spent fuel pool and dipping in the alloy, ideally. After the neutron-poisoning alloy has been applied, the fuel rods would be placed in dry cask storage. It is understood that this process would involve alterations to the current procedure for transferring fuel bundles; however, solving those issues is outside the scope of this project.

The scope of this project entailed experimental verification, analysis of heat transfer properties, calculations of the effects on k_{eff}, and finally a simple, materials cost analysis of adding an alloy to current zircaloy fuel rods. It is inherently understood that regulatory requirements are not considered this early in the design process. Furthermore the scope of this project does not include analysis of alloy adherence to areas of thermal expansive or radiation creep induced stress cracking on the surface of the fuel rods. Similarly, the effects of hydrogen build-up from normal operation, heat-induced reactions of zirconium and water are not considered in this analysis.

To begin the project an alloy was chosen based on several criteria, discussed below. With a selected alloy, experiments were conducted to verify the ability of the alloy to adhere to the rod surface. All attempts were documented with failures being discarded and possible successful samples saved for further investigation. Initial criteria for keeping a sample included simple stress tests and visual inspection. Further analysis was conducted using a microscope for surface examination. This was followed by close examination of the alloy-to-rod interface, which was made possible by cutting through the rod and coating perpendicular to the rod's central axis. These processes are described in further detail in the following sections.

Three characteristics were used as guidelines while selecting an alloy for investigation as a possible candidate for use as a spent fuel pin and/or bundle coating. Logically, the material must be economically advantageous, and for usefulness, it must be an effective neutron poison. In order to provide reliable integrity, a high enough, yet realistically manageable for operational purposes, melting point is necessary to prevent melt-off during storage caused by decay heat. Common structural dipping alloys are used at temperatures as high as 450 °C[7]. Thus past experience shows that relatively high temperature dipping is viable in the work place. A final decision was made to use a 60 Zn-40 Cd mixture as it satisfactorily met the four criteria. The alloy melts at approximately 335 °C and has a high neutron absorption cross section. Both cadmium and zinc are relatively cheap, making the alloy a strong candidate with respect to economics. The primary disadvantages of the alloy choice included the toxic nature of cadmium, overlooked due to the much higher danger of dealing with spent nuclear fuel, and the uncertainty of whether or not it was possible to have an alloy adhere to zirconium. Experiments were done to prove that the alloy could wet to a Zircaloy-4 rod.

Experimental Methodology

In order to prove that this alloy is viable, several small-scale experiments were conducted. The alloy was heated until sufficiently melted, just above the melting point of 335 °C, and then a clean zircaloy rod was dipped in the alloy. The apparatus used for melting and dipping the rods is shown in Figure 7.

Figure 7 Experimental Setup

This procedure was repeated with an increase in both temperature and time with varying amounts of success. If the alloy appeared to have wet the rod, the specimen was put aside for cooling and further closer examination. Initial experiments were performed without rod-surface preparation. After confirming all of these cases to be failures the next step was to employ surface preparation.

The rod surface was prepared for dipping using three different processes. Two different fluxes were used as well as an acid dip preparation. The flux providing best results was Ultra-flux II, provided by Dr. M. L. Grossbeck. The highest alloy temperature used in conjunction with the flux was 480 °C, with our best results occurring at 473 °C. A single sample was retained using the Ultra Flux II at 473 °C. All other samples from the flux preparation experiments were discarded as failures. For the final experiment, an acid dip composed primarily of nitric acid with small amounts of hydrofluoric acid was used to clean and etch the rod surface before dipping. Initially, the alloy did not adhere to the rod, much like the earlier failed attempts. In order to overcome the dislocation energy of the rod's surface atoms, the alloy temperature was steadily increased. In theory, dislocation of surface atoms allows the alloy atoms to act as interstitials in the zircaloy lattice. At 650 °C the alloy adhered to the zircaloy surface very well, hinting at success. A detailed discussion on the successful specimens is given in the results section. The acid dip provided better results than flux application, however the alloy temperature may have

been the major contributing factor. More experimentation is needed to verify the true cause of success. With several specimens coated in alloy that was not removable by force, the next step was examination.

Alloy Coating Results

After approximately 25 experiments, three samples required further examination. The following descriptions progress in order of importance with the least important sample described first.

The first sample was dipped without surface preparation at an alloy temperature of approximately 340 °C. Visually, the sample appeared to have areas of adherence on the molecular level. However, after application of force in areas with visible gaps between the coating and rod, the alloy was removed indicating this sample's alloy did not adhere to the surface on a molecular level. It is hypothesized that the reason the alloy stuck to the rod is a matter of simple heat transfer. The rod, at room temperature, was inserted into the alloy at temperatures very close to the melting point. The temperature differential between rod and alloy caused energy to be quenched from the alloy material immediately around the rod. The loss of energy was significant enough to solidify the alloy creating an incasing covering on the outside of the rod. The rod was removed from the melting pot before the coating layer had ample time to melt back off of the zircaloy rod. It is assumed that given ample time and heat, the alloy coating and rod would have reached the alloy melting temperature and the alloy would have fallen away from the rod without any coating. This is in contrast to true adherence where the alloy atoms would have become interstitials in the zircaloy surface lattice and been permanently applied. The sample discussed is shown in Figure 8.

Figure 8 Sample without surface preparation at 350 °C after alloy has been partially removed by force

The second sample set aside for further examination was created using the Ultra Flux II surface preparation and dipped in the alloy at 473 °C. After application of the flux the rod sample was dipped into the alloy and allowed to sit for 2 minutes. This time was required for the flux to visually boil off of the rod surface allowing the alloy to come into contact with the rod. Upon removal of the sample it was apparent that the alloy had dried onto the flux but had not penetrated the flux sufficiently enough to interact with the rod. This was verified by scraping the coating off with minimal effort. With the alloy removed, a thin layer of flux was left on the rod's surface. The remaining flux was sufficient to prepare the surface for dipping. The rod was dipped back into the alloy at 473 °C without further preparation assuming that no other flux was necessary. The thin layer of flux was boiled off relatively quickly and, after about 1 minute, the rod was removed. The majority of the alloy was removed with minimal force, however, some of the alloy was not easily removed and this became our first example of possible adherence on a molecular level.

To verify the coating, the sample was cut perpendicular to the central axis through the coating alloy using a high-speed circular saw. A diagram of the cut is provided in Figure 9.

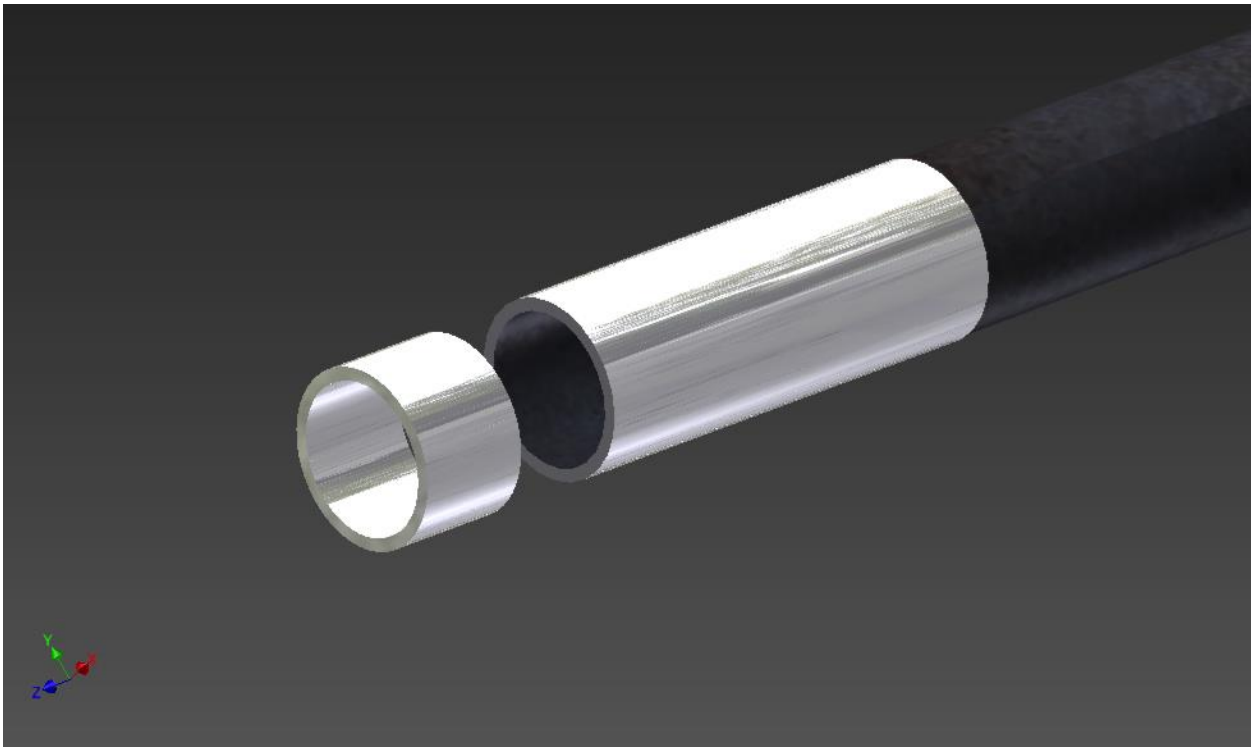

Figure 9 Diagram of rod after being cut for examination

This provided a vantage point from which the alloy-to-rod interface could be examined. Under microscope examination the alloy proved to have both areas of failed and successful wetting. The success was proven by the inability to identify a gap between the alloy and rod. The sample before cutting is shown in Figure 10.

Figure 10 Sample using Ultra Flux II and dipped at 473 °C

The final sample was prepared using an acid bath and then dipped into the molten alloy at 650 °C. The rod was allowed to soak in the acid for approximately 5 minutes before rinsing in tap water and placement in a plastic bag. Afterwards it was carried to the lab and the dipping process began. Initial low temperature dips resulted in no success; however, after increasing the alloy temperature to 650°C the alloy stuck to the rod and could not be removed through applied force. Validation was done on the second sample using a scanning electron microscope (SEM), which allowed ultra-close examination. The sample before imaging was conducted is shown in Figure 11. From 500 to 1500x magnification it became very clear that the alloy bonded to the rod on a molecular level, as shown in Figures 12-14 which were taken using the SEM.

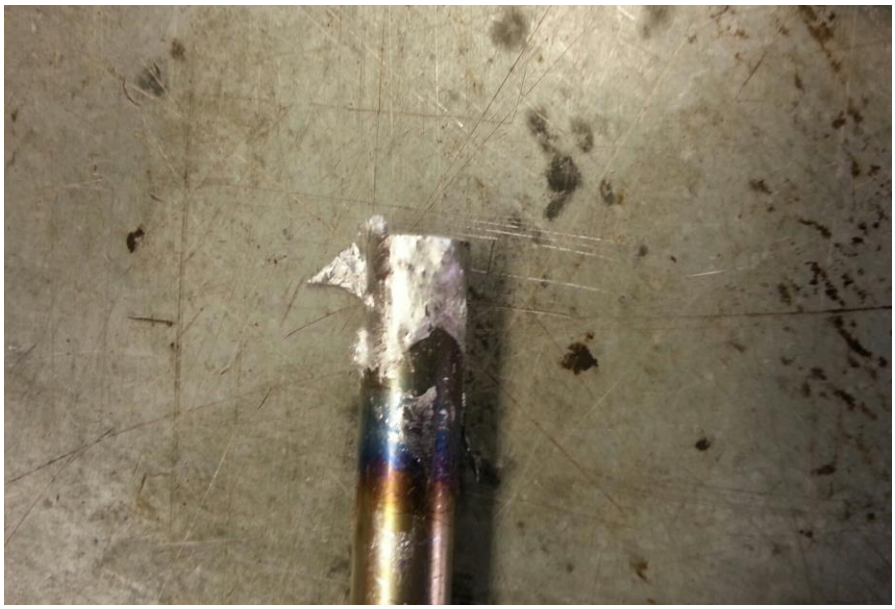

Figure 11 Alloy coating on zircalloy with acid preparation and alloy temperature of 650 °C

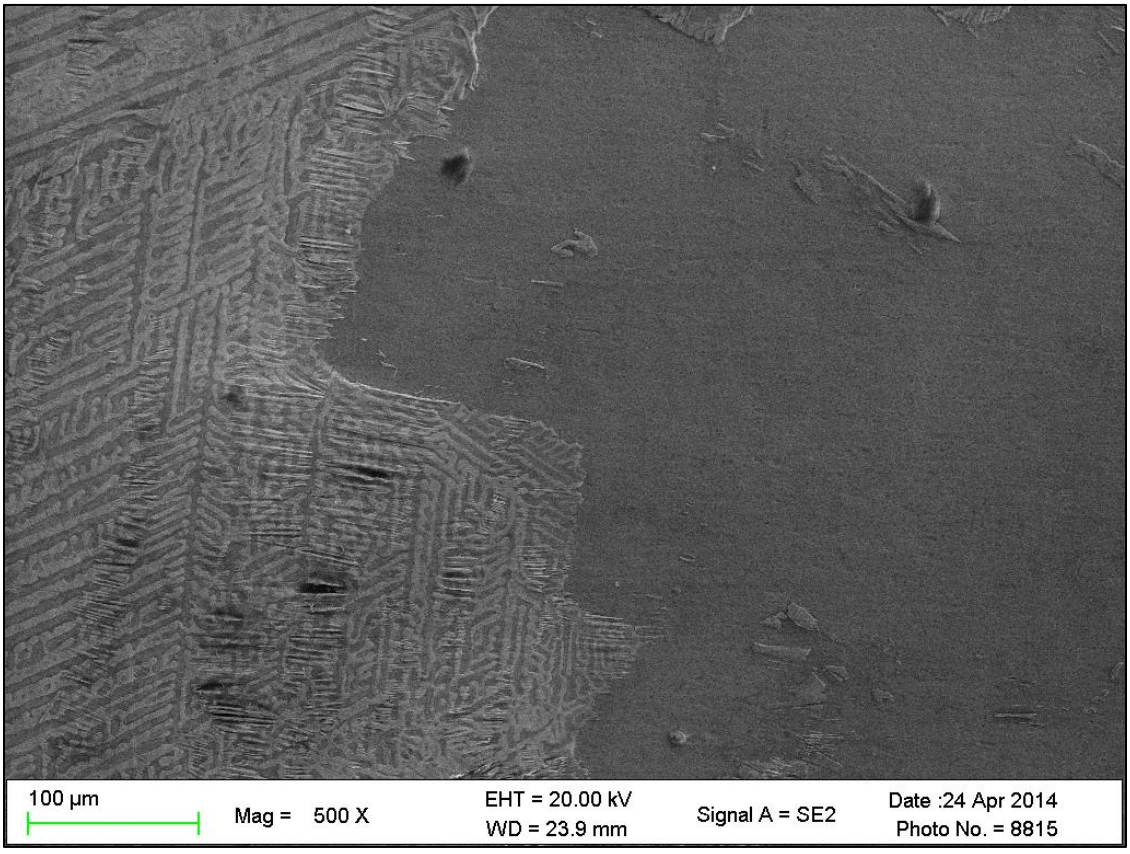

Figure 12 Image of the coating alloy and rod interface at 500x

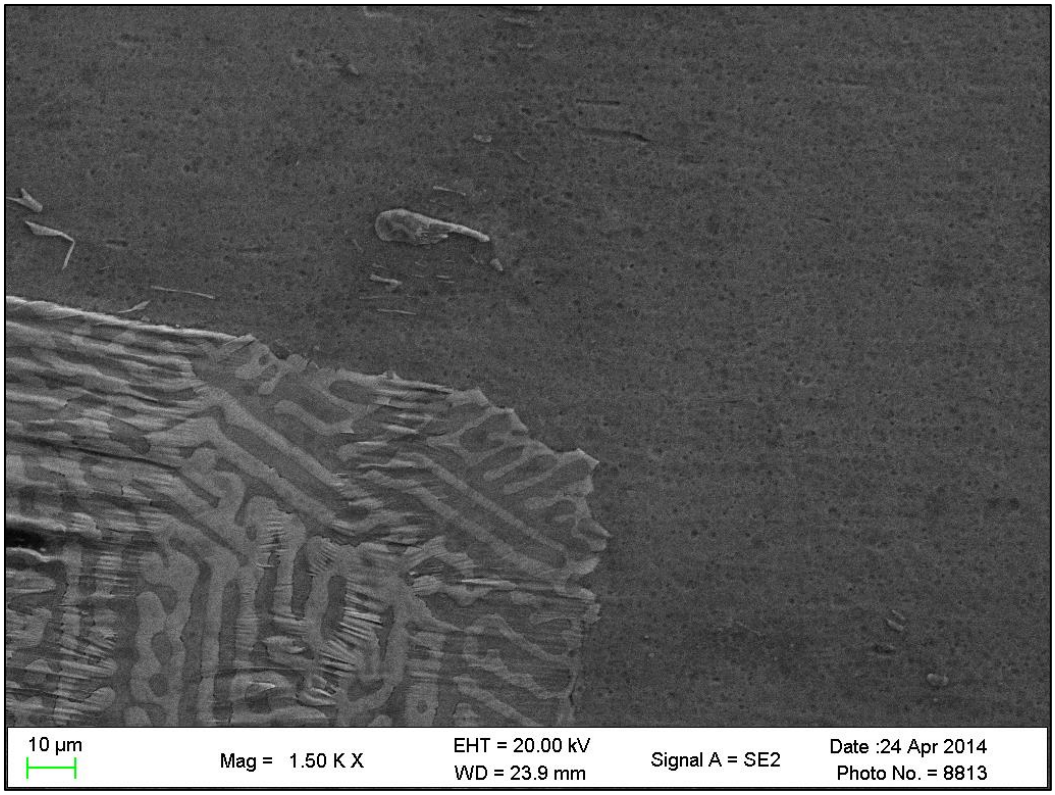

Figure 13 Image of the coating alloy and rod interface at 1500x

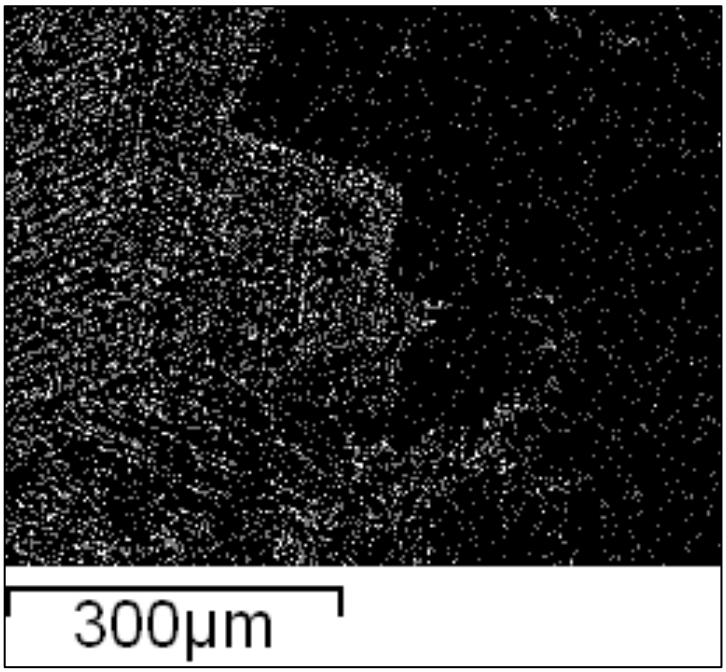

Figure 14 SEM Image of alloy/rod interface with cadmium highlighted

After measuring the thickness of the achieved coating, it became possible to calculate the neutron attenuation and thus validate the alloy's ability to reduce k_{eff}. The code of choice for k_{eff} calculations was the popular Monte-Carlo software SCALE.

K_{eff} Calculation Methodology

The goal of the alloy coating is to increase the efficiency of the used nuclear fuel pool storage system. It can be reasonably inferred that the neutron poison coating would reduce the multiplication factor, k_{eff}, by a considerable amount, allowing for more fuel bundles to be stored in a pool or in dry storage. This would allow for a reduction in the per-unit cost of storing used nuclear fuel. It becomes prudent to consider how the alloy dip will change the neutron population behavior. A 3x3 array of typical PWR assemblies (17x17 rods) was modeled in SCALE6.1[1*] using the CSAS25 and NITAWL sequences. The first case considered had the standard materials found in a fuel assembly of lightly enriched UO_2 fuel with zircaloy cladding and water surrounding the assemblies. Next, varying alloy coat thicknesses were considered, in increments of 0.0002 centimeters. Then, the same thickness was tested with the molten salt solution filling the space between rods, as well as a case with helium, and a case with air. The helium is considered to be similar to a dry cask storage system, and for thoroughness, the air case was considered to simulate a scenario in which coolant had boiled off. However, it is the group's belief that with a lack of coolant, the fuel would melt, causing a significant change in the geometry of the fissile material, meaning this particular simulation run does not model a realistic situation. Overall, the preliminary calculations show that the solder dip in a water pool behaves as expected, with a decaying exponential marking the behavior of k_{eff} as the solder thickness increases.

The value of k_{eff} for the initial case was calculated to be 0.8469 ± 0.0013. While this is just a representative case of several assemblies in a pool, this number serves as a control value for making comparisons. When the only change made was the dip being applied for the water pool at a thickness of 0.0002 centimeters, the k_{eff} was calculated to be 0.6037 ± 0.0010. This is a significant reduction, confirming that a very thin layer of the alloy coating is quite effective. This

[1]* SCALE6.1 (ORNL/TM-2005/39, Oak Ridge, TN, 2011)

thickness remains the same for the following cases. The next case considered is that of the molten salt pool. When the water of the pool is replaced with the mixture of the molten salt pool, the k_{eff} is reduced again, this time to 0.19066 ± 0.00050. This reduction can be explained by the neutron collision and moderation mechanics. The Hitec salt mixture is modeled as 47.67 wt% oxygen, 20.50 wt% potassium, 16.62 wt% nitrogen, and 0.1522 wt% sodium. None of these elements are particularly known for their capabilities as a thermal neutron moderator. It is possible the salt's lack of the hydrogen, which water possesses, causes a significant reduction in the energy loss mechanics needed for a sustained thermal fission chain reaction.

However, further research is suggested to examine whether this is due to shielding, absorption resonances, or under-moderation. Another consideration is the area of applicability of the model. Thus far, there is not a lot of data on the behavior of low-temperature molten salts as moderators. As such the validation of such a model is still quite lacking. Shown below in Figure 15, the k_{eff} of the alloy is compared between a few of the considered models.

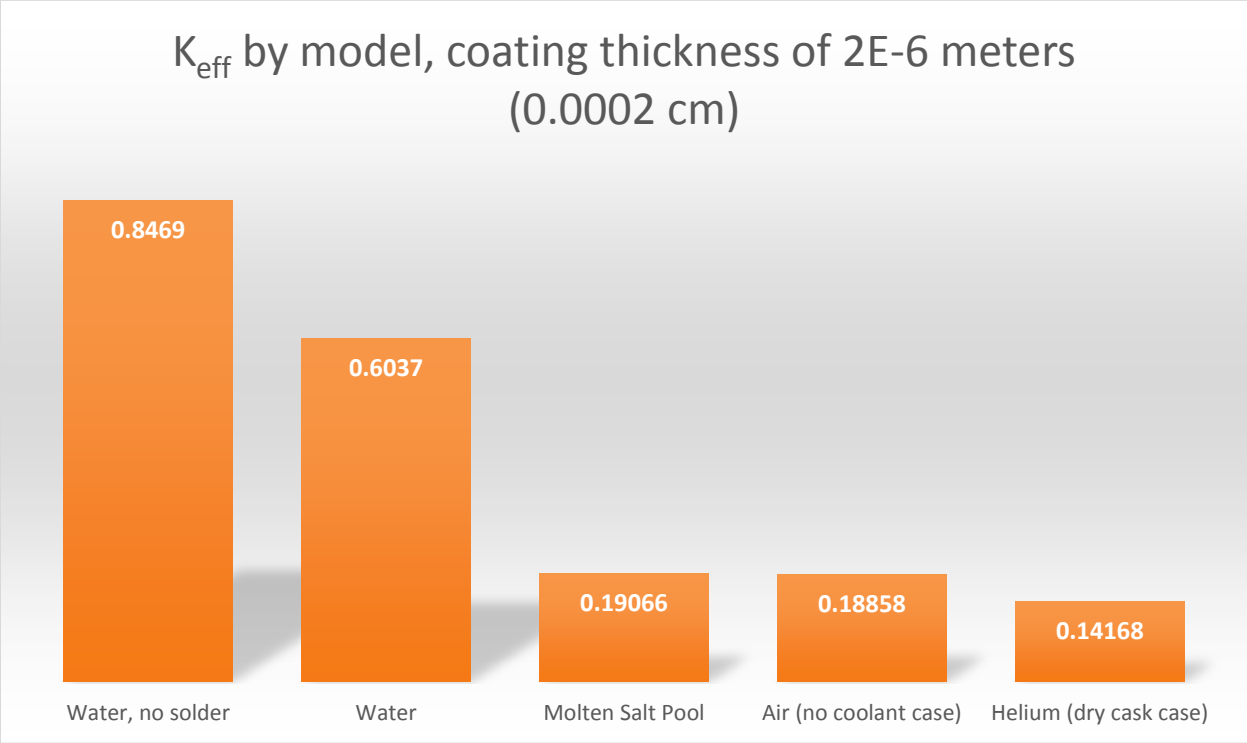

Figure 15 Simulation results for K_{eff} calculation

Due to a lack of cross-section data for zinc in SCALE, the material was replaced with aluminum. This choice is a conservative change, as aluminum has a small neutron interaction cross-section

compared to cadmium. The thought is that by using aluminum, the only absorptions will be from the cadmium present. If data becomes available, these calculations should be repeated with the correct material specification. One of the input decks used for this modeling can be found in the appendices section. The only changed value for each run is the radius of the coating alloy unit. For the salt pool, the h2o card is changed for a weight percent composition of the constituent elements of the homogeneous molten salt mixture. Similarly, for the air and helium cases, the material specifications are changed.

Thermal Analysis

Before an alloy coating can be applied to a used fuel assembly, one must ensure that the system maintains removal of decay heat from the fuel sufficient to prevent heat up and damage. For this reason, a model was constructed using COMSOL[2*] Multiphysics to demonstrate the steady state temperature of a used fuel assembly both with and without a 60Zn-40Cd coating. A single 17X17 fuel assemble was considered with geometry being as described in Table 7 below. To simulate fuel roughly 5 years after removal from core (a typical in-pool time before transfer to dry cask), a decay heat generation of 2 kW/tonne was chosen based on Figure 16, below.

[2]*COMSOL 4.3b (COMSOL Inc., Palo Alto, CA, 2013)

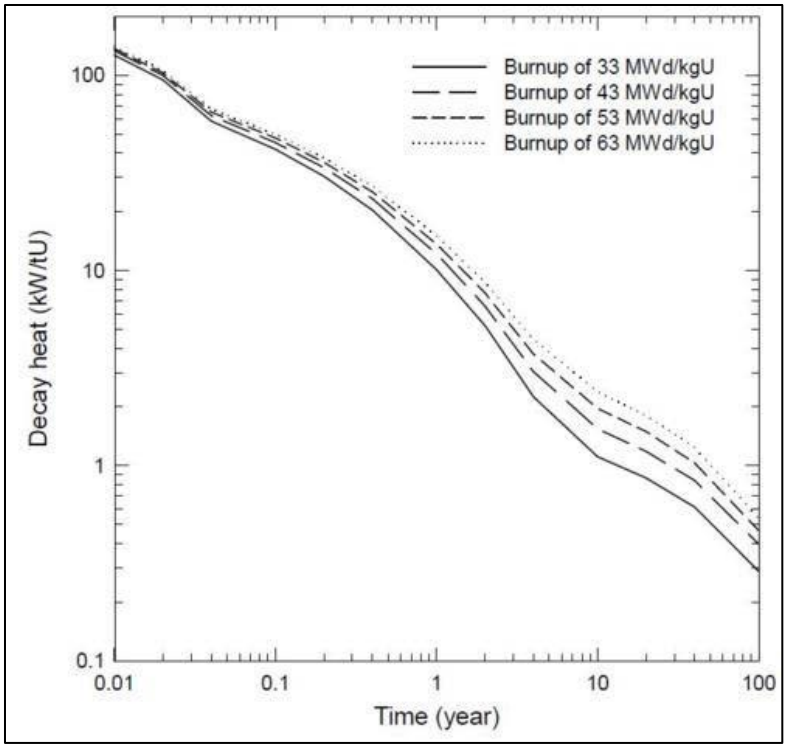

Figure 16 Decay heat of used fuel assemblies over time[9]

Geometry of a Fuel Array	
Fuel Diameter	8.2 mm
Cladding Thickness	0.57 mm
Total Rod Diameter	9.34 mm
Rod Height	4 m
Rod Array	17 x 17
Rod Centerline Separation	12.6 mm
60Zn-40Cd Coating Thickness	0.0254 mm

Table 7 Geometry of fuel array modeled[10]

For ease of calculation, a two dimensional model of a single fuel assembly with no support structure was considered. In the model, it was assumed that the assembly is lying horizontally (with rod axis perpendicular to the local gravitational field) to simulate conditions in final dry cask storage. For conservatism, all 289 rods were considered to be heat generating, i.e. no control rod sites were placed in the fuel array. To further simulate a dry cask environment, natural

convection to a helium environment is considered as the primary form of heat removal. Figure 17 shows the steady state temperature distribution within this fuel array, while Figure 18 shows the same for a fuel assembly with a 0.0254 mm (0.001 in.) coating of 60Zn-40Cd alloy placed around the cladding, corresponding to the thickness of coating that was experimentally deposited on zircaloy.

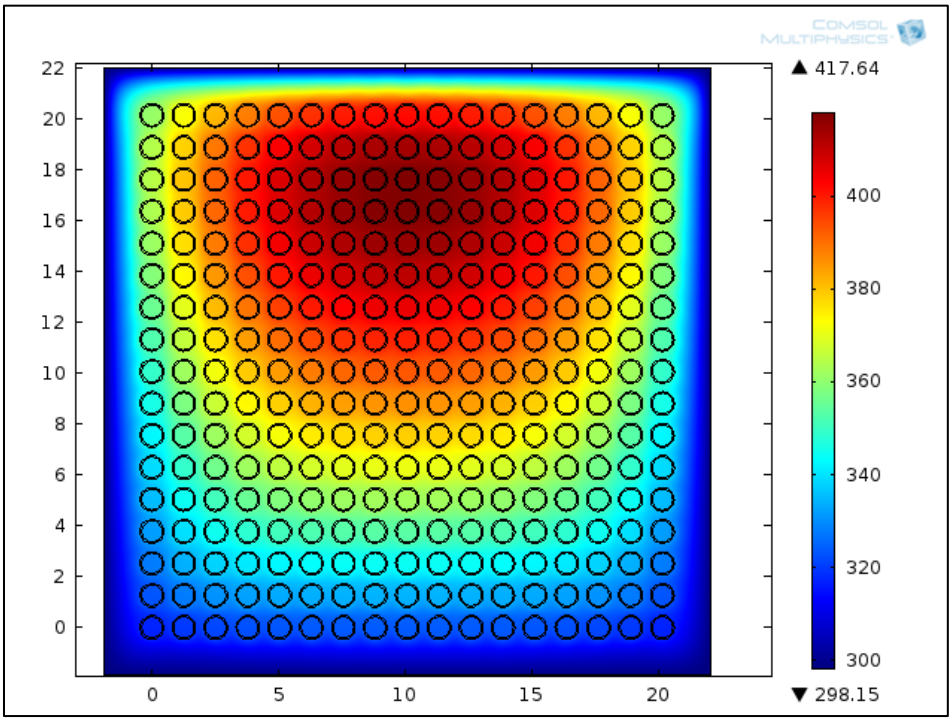

Figure 17 Steady state temperature in horizontally lying used fuel assembly with no coating (in K)

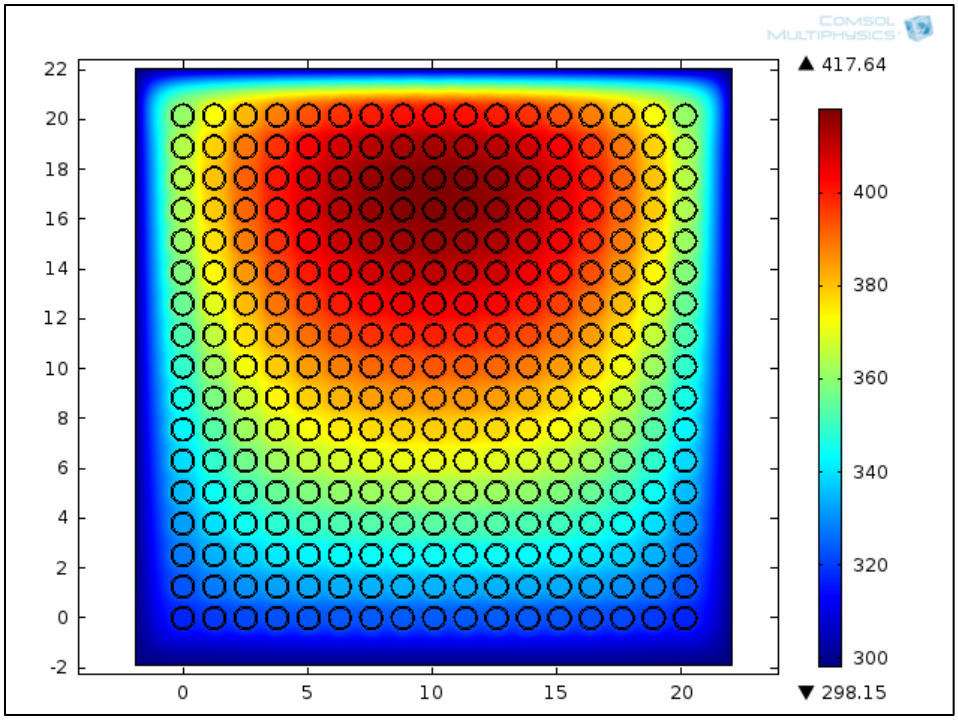

Figure 18 Steady-state temperature in horizontally lying used fuel assembly with 0.0254 mm 60Zn-40Cd coating (in K)

It can be seen from Figures 17 and 18 the addition of a thin layer of alloy on the exterior of the cladding caused no change in the temperature distribution in the fuel assembly, with both having maximum steady state temperature of 418 K (145 °C). As such, it can be concluded that a thin alloy coating on fuel assemblies would cause no temperature concerns in current dry cask arrangements. Another simulation was then carried out to test the effect of compacting the array to allow space for more rods. An array of similar coated rods is considered in which the centerline-to-centerline separation has been reduced by 10% to 11.34 mm. Such a decrease in separation would allow for an 18x18 array of rods to be placed in the same area; however, for the sake of comparison, a 17x17 array is considered in this model. The results can be seen in Figure 19 below.

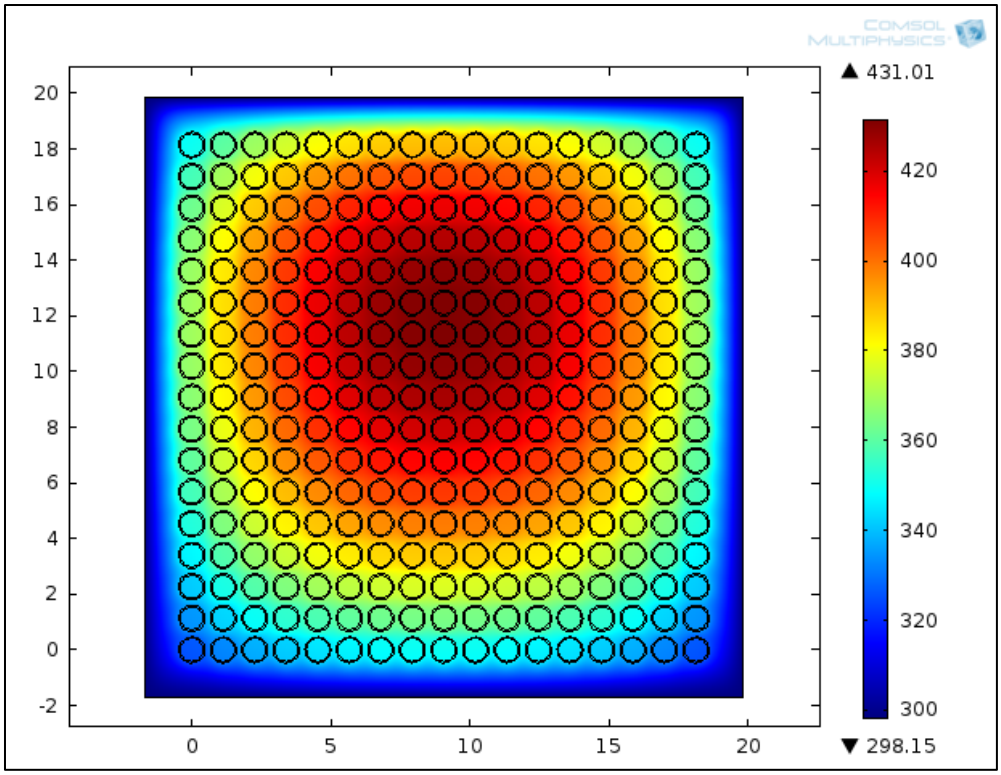

Figure 19 Steady-state temperature in horizontally lying used fuel assembly with 0.0254 mm 60Zn-40Cd coating and reduced rod separation (in K)

In this model, it can be seen that the reduction in rod spacing increased the maximum temperature in the assembly to 431 K (158 °C). This 3% increase is not considered substantial, but it is possible that such an increase could create concerns if the entire cask were considered and not just a single assembly. Such an increase could be further problematic if the extra space created by compacting were filled with more used fuel rods. Thus, while it appears that such compacting is possible, it cannot be recommended until a full dry cask model is studied. Although the authors were not able to model the full dry cask due to computational limitations, it is suggested that a three-dimensional, fully-coupled computational fluid dynamics (CFD) and heat transfer simulation be carried out to consider the steady state temperature in a full dry cask array as seen in Figure 20 below.

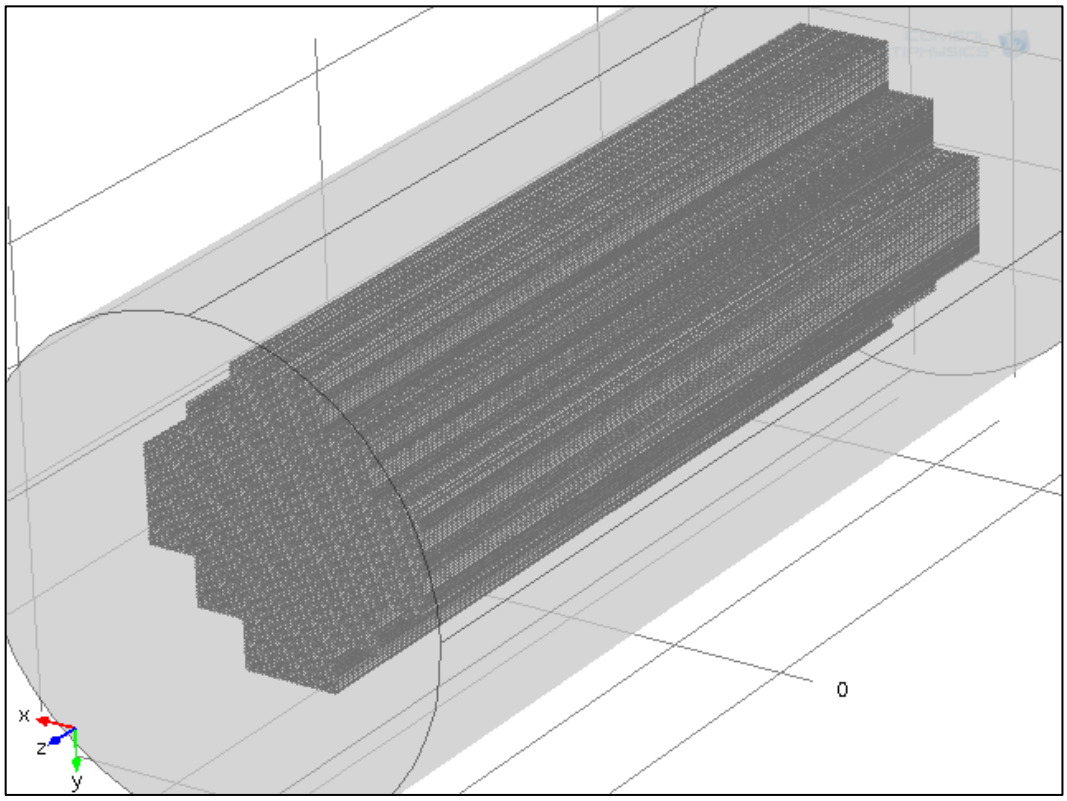

Figure 20 Proposed geometry for future full cask thermal simulation

Cost Analysis

In order to better understand the total impact of the proposed solutions, a cost analysis was conducted and compared to current technology. Table 8 lists the approximated costs of materials for the solutions put forth in this paper.

Material	Cost ($)
Hitec	1.793 million
Water (at $.005/gallon for 240,000 gallons)	1,196.88
Cadmium (per bundle)	930.31
Zinc (per bundle)	88.25
Total cost per bundle	1,018.56
Total cost for Dry Cask (24 bundles)	24,445.44

Table 8 Cost analysis of Hitec spent fuel pool and 60Zn-40Cd coating

For the purpose of the spent fuel pool, the construction costs were assumed to be similar to how SFP are traditionally built with Hitec salt pool using current dimensions of SFP. The volume of an average spent fuel pool is approximately 32,000 ft^3. To fill this amount of volume with Hitec salt would be about $1.8 million dollars if the cost is commercially available at approximately $1/kg. It is possible that this cost could be reduced due to the incredibly large amount required and the following assumption that the cost would be 50% - 75% of this approximated price. This change would then reduce total cost to fill the spent fuel pool to approximately $900,000 to $1.35 million. The amount of water required fill a spent fuel pool would require 240,000 gallons, and at a commercially available price of $.005 per gallon for water, the pool would cost approximately $1,196.88. This is assuming KUB tap water price but included is the assumption the water would pass through an ion exchanger and demineralizer before the spent fuel bundles are added. After this proper chemical treatment would be performed to ensure purity of the water is maintained at a pH of 7.0. Even with these extra steps taken and a deep discount of the Hitec salt, the economic cost of replacing water with the Hitec salt would have to be left to the discretion of the investors of the SFP. The increase in safety of replacing the water with the Hitec cannot be discounted, though. With the increase in regulations from the Nuclear Regulatory Commission and with the decrease in positive public opinion, the possible cost of not taking steps to increase safety could cause a loss in investment of the shareholders. With a

higher upfront cost of material but a loss of skepticism and critical public and government opinion, the plant could operate with less unforeseen costs due to better systems in place to ensure accidents such as the Fukushima event are adverted.

The cost of each bundle was determined based upon the following assumptions. The amount of coating required for each fuel rod is .254 mm with the length of each fuel rod assumed to be 4 meters in length. A fuel bundle consists of a 17 x 17 fuel rod matrix. The coating is made of 60% Zinc and 40% Cadmium and this was then used to find cost per fuel bundle. The market cost of zinc is approximately $0.93 per pound, whereas the market price of cadmium is $12.00 per pound. These prices will fluctuate and can be lowered depending on the amount obtained from the distributor. With these current market prices assumed, it would require around $1018.56 to coat each fuel bundle. The breakdown of this cost comes from $88.25 of zinc and $930.31 of cadmium. There are 24 fuel bundles per dry cask, so the cost of coating all fuel bundles for a dry cask would amount to $24,445.44.

In theory, the coating of spent fuel bundles before dry cask storage allows the spent fuel to be placed in a tighter geometry than was originally assessed. As previously stated, there is a potential for temperature concerns in such a configuration, but if possible, this would create an interesting saving for the power plant investors. If the ability to package fuel closer together allows for at least one or two more fuel bundles to be safely placed in a single dry cask, the reduction of just two dry casks completely covers the cost of the Hitec molten salt expenditure mentioned above. This will have a twofold affect. Since it would be possible to reduce the required amount of dry casks needed for spent fuel storage, thus increasing profits by reducing expenditures, it will also increase safety and public opinion of the plant as stated above. Once again the increase in public opinion and ease of regulation from government entities could translate to higher profits and larger returns on investment. This would be a win-win situation for all stakeholders involved with the nuclear power plant. Once this design is perfected and the possible redesign of dry storage cask is complete, the ability of the company who implements these designs could easily gain footholds in new markets. This change would increase profits due to the increased safety margin and decreased resistance from residents in the area which would allow for ease of construction of new plants in new areas. A dry cask storage amount was

considered due to the increasing amount of fuel bundles being placed in wet storage from change in storage geometry thus increasing the amount of fuel bundles being stored in a pool.

Conclusion and Future Work

At present, the group's work suggests plausible solutions to the two challenges presented. A molten salt based spent fuel pool consisting of the commercial salt Hitec ensures a significantly longer time to coolant failure in the case of accident conditions when compared to conventional, water spent fuel pools. Additionally, the simulations show that a fuel pool filled with Hitec has a lower k_{eff} than a pool filled with water. This fact combined with the dramatically increased safety margin in the time it takes the pool to reach a failure temperature might allow for tighter packing of fuel inside of the SFP. Furthermore, it has been demonstrated a thin coating of a 60 Zn-40 Cd alloy can be placed on the outer edge of spent fuel rods via dip soldering in order to act as a neutron absorber. Preliminary results indicate that only a thin layer of the material is needed to create the amount of shielding necessary to prevent criticality and that such a layer is achievable via conventional dip soldering methods. Analysis shows that a layer of the Zn-Cd alloy does cause the spent fuel to reach higher temperatures, but it is not expected that the increase is enough to cause problems, and work is underway to test this hypothesis.

As such, future work must be performed to scale this dip soldering process to an industrial level. Currently, large-scale dip soldering is commonly performed in many industrial applications, but this process must be adapted for use in nuclear power plants. Furthermore, concerns have been raised regarding the condition of the cladding on spent fuel elements as compared to that of clean zircaloy. Further research is needed to ensure the viability of coating to such damaged zircaloy or to prescribe a viable method in which the cladding may be restored to a clean condition before the coating is administered.

References

1. Robert Alvarez , Jan Beyea , Klaus Janberg , Jungmin Kang , Ed Lyman , Allison Macfarlane, GordonThompson & Frank N. von Hippel (2003) *Reducing the Hazards from Stored Spent Power-Reactor Fuel in the United States,Science & Global Security: The Technical Basis for Arms Control, Disarmament, and Nonproliferation Initiatives*, 11:1, 1-51, DOI: 10.1080/08929880309006

2. US Nuclear Regulatory Commission. (1997). Operating Experience Feedback Report Assessment of Spent Fuel Cooling. *NUREG-1275, 12*.

3. Coastal Chemical Co., L.L.C. (2004, July 20). *Hitec Salt*. [Material Safety Data Sheet].

4. Coastal Chemical Co., L.L.C. *HITEC Heat Transfer Salt*. Accessed via email communication with T. Brace 2014, March 27.

5. Schmidt, F. W., Henderson, R. E., & Wolgemuth, C. H. (1984). *Introduction to Thermal Sciences: Thermodynamics, Fluid Dynamics, Heat Transfer*. Wiley.

6. ORNL Heat Transfer Salt for Steam Generation ORNL-TM-3777

7. Steel Construction.info. *Metallic Coatings.* (http://www.steelconstruction.info/Metallic_coatings)

8. E. D. Throm, NUREG-1353 (April 1989).

9. A. Sowder, *Wet Storage of Used Fuel*, University of Tennessee Lecture (Unpublished).

10. N. E. Todreas and M. S. Kazimi, *Nuclear Systems 1: Thermal Hydraulics Fundamentals*, 1st Ed. (Taylor & Francis, New York, NY, 1990). pp. 12-15.

11. D. Wilkie, SPENT FUEL POOLS AT FUKUSHIMA FOLLOW ON REPORT "CORROSION" (Dec 2012) http://www.fukuleaks.org/web/?page_id=8544

Appendix

Appendix A: Matlab code used for thermal analysis for the spent fuel pool

```
%% Pool Heat Up Calculator
% UTK, NE 472: Senior Design
% This program promtps the user for a heat generation term and returns the
% time to boiling or reaching maximum operating temperature for a pool of
% water or Hitec, respectively.

clear all, close all, clc, format compact;

%% constants
T_film_air=30;
TinfAir=30;
T_wall=30; %constant wall temp at a depth of...
L_w=5; %m
k_w=1.4;
g=9.81;
sigma=5.67e-8; %w/m2-K4

%% Properties of pool
L_p=12.19;
W_p=9.14;
H_p=7;
V_p=906; % this is  using 32000 ft^3 given by NRC Doc
emiss_water=.96;
emiss_hitec=.3; % Conservative aproximation using reference value at .4

%% prompt user for heat input
prompt={'Enter Heat Generation (btu/hr)'};
dlg_title='Input';
inflow_eng=inputdlg(prompt,dlg_title); % in btu/hr
inflow_eng=str2double(inflow_eng);
inflow=inflow_eng*.2931; %Watts

%% some properties of the coolants
T_boil_water=100;
T_boil_hitec=800;
T_max_hitec=538; %degC


%% Set up Temp and time vectors
dT=.25;
Ti_water=125; %degF
Ti_water=(Ti_water-32)/1.8; % degC
T_wall=Ti_water;
Ti_hitec=160; %degC
T_wall_hitec=Ti_hitec;

T_pwater=[Ti_water:dT:T_boil_water];
```

```
T_phitec=[Ti_hitec:dT:T_max_hitec];
% these will be in seconds
t=0;

%% calculate time/temp changes
for i=[1:length(T_pwater)-1]
    T_film_air=(T_pwater(i)+TinfAir)/2; %use film temperature
    T_film_p=(T_pwater(i)+T_wall)/2;

    % find thermophys properties
    %% Air Thermo Physicals from Air Film
    beta_air=1/(T_film_air+273);
    cp_air=-7.357*10^-7.*T_film_air.^3+.0007039.*T_film_air.^2-...
        .006618.*T_film_air+1004;
    pr_air=2.823*10^-7.*T_film_air.^2-.0002107.*T_film_air+.7183;
    nu_air=9.312*10^-11.*T_film_air.^2+8.591*10^-8.*T_film_air+1.358*10^-5;
    k_air=-2.183*10^-8.*T_film_air.^2+7.755*10^-5.*T_film_air+.02399;
    rho_air=8.955*10^-11.*T_film_air.^4-7.269*10^-8.*T_film_air.^3+...
        2.206*10^-5.*T_film_air.^2-.004725.*T_film_air+1.263;

    %% Water Thermo Physicals from pool Film

    rho_water=1001.1-.0867.*T_film_p-.0035*T_film_p^2;
    k_water=.5636+1.946*10^-3*T_film_p-8.151*10^-6*T_film_p^2;
    beta_water=7.957*10^-5+7.315*10^-6*T_film_p;
    cp_water=(4.214-2.286*10^-3*T_film_p+4.991*10^-5*T_film_p^2-...
        4.519*10^-7*T_film_p^3+1.8567*10^-9*T_film_p^4)*1000;
    mu_water=1.684*10^-3-4.264*10^-5*T_film_p+...
        5.062*10^-7*T_film_p^2-2.244*10^-9*T_film_p^3;
    nu_water=mu_water/rho_water;
    Pr_water=cp_water*mu_water/k_water;
    %% Test Beta Water

    water_Ref_Dens=1001.1-.0867.*Ti_water-.0035*Ti_water^2;
    mwater=water_Ref_Dens*V_p;
    water_Ref_Temp=Ti_water-1;
    water_Ref_Vol=mwater/water_Ref_Dens;

    water_vol=mwater./rho_water;
    beta_water_test=(water_vol-water_Ref_Vol)...
        /(water_Ref_Vol*((T_film_p)-65));

    %% calc heat transfer coefficients water case

    % nat conv: pool to wall
    Gr=(g*beta_water*(T_pwater(i)-T_wall)*H_p^3)/nu_water^2;
    Ra=Gr*Pr_water;
    sci=(1+(.492/Pr_water)^(9/16))^(-16/9);
    if (Ra<10^9)
        Nu=.68+.67*(Ra*sci)^(1/4);
    else
        Nu=.15*(Ra*sci)^(1/3);
    end
    h_nw=Nu*k_water/H_p;
    A_ht=2*H_p*(L_p+W_p);
```

```
    Q_nw=(T_pwater(i)-T_wall)/(L_w/k_w/A_ht+1/h_nw/A_ht); %with conduction

    %nat conv: pool to air
    L_c=L_p*W_p/(2*L_p+2*W_p);
    Gr=(g*beta_air*(T_pwater(i)-TinfAir)*L_c^3)/nu_air^2;
    Ra=Gr*pr_air;
    if (Ra<10^7)
        Nu=.54*Ra^(1/4);
    else
        Nu=.15*Ra^(1/3);
    end
    h_na=Nu*k_air/L_c;
    Q_na=h_na*(L_p*W_p)*(T_pwater(i)-TinfAir);

    % radiation from top
    Q_ra(i)=sigma*emiss_water*((T_pwater(i)+273)^4-...
        (TinfAir+273)^4)*W_p*L_p;

    mwater=rho_water*V_p;
    % time change
    Qout_Water=Q_nw+Q_na+Q_ra;

    dt=mwater*cp_water*dT/(inflow-(Q_nw+Q_na+Q_ra(i)));
    t(i+1)=t(i)+dt;

end

HoursWater=t/3600; % convert to minutes
Time_to_boil_water=HoursWater(length(HoursWater)) %display result

%% do the calc for hitec

t_hitec=0;

%% calculate time/temp changes

for m=[1:length(T_phitec)-1]
    T_film_air_hitec=(T_phitec(m)+TinfAir)/2; %use film temperature
    T_film_phitec=(T_phitec(m)+T_wall_hitec)/2;

    % find thermophys properties
    %% Air Thermo Physicals from Air Film
    beta_air_hitec=1/(T_film_air_hitec+273);
    cp_air_hitec=-7.357*10^-7.*T_film_air_hitec.^3+...
        .0007039.*T_film_air_hitec.^2-.006618.*T_film_air_hitec+1004;
    pr_air_hitec=2.823*10^-7.*T_film_air_hitec.^2-...
        .0002107.*T_film_air_hitec+.7183;
    nu_air_hitec=9.312*10^-11.*T_film_air_hitec.^2+...
        8.591*10^-8.*T_film_air_hitec+1.358*10^-5;
    k_air_hitec=-2.183*10^-8.*T_film_air_hitec.^2+...
        7.755*10^-5.*T_film_air_hitec+.02399;
    rho_air_hitec=8.955*10^-11.*T_film_air_hitec.^4-...
        7.269*10^-8.*T_film_air_hitec.^3+2.206*10^-...
        5.*T_film_air_hitec.^2-.004725.*T_film_air_hitec+1.263;
```

```
    %%  Hitech Thermo Physicals
    rho_hitec=(2.084-7.4e-4*T_film_phitec)*1000;

    cp_hitec=1560;
    k_hitec=.411+1.54e-6.*T_film_phitec^2+4.36e-4.*T_film_phitec;
    nu_hitec=(T_film_phitec.^(-2.104))*10^5.7374; %cp unit;
    Pr_hitec=nu_hitec.*cp_hitec./k_hitec;
    % stuff to calc beta

    Hitec_Ref_Dens=(2.084-7.4e-4*141)*1000;
    mhitec=Hitec_Ref_Dens*V_p;
    Hitec_Ref_Temp=141;
    Hitec_Ref_Vol=mhitec/Hitec_Ref_Dens;
    Density_Hitec=(2.084-7.4e-4*T_film_phitec)*1000;
    Hitec_vol=mhitec./Density_Hitec;
    %beta_hitec=beta_water

    Deltaforbeta=T_film_phitec-141;

    beta_hitec=(Hitec_vol-Hitec_Ref_Vol)/(Hitec_Ref_Vol*((T_film_phitec-
141.9)));

    %% calc heat transfer coefficients water case
    beta_airhitec=1/(T_film_air_hitec+273);

    % nat conv: pool to wall
    Gr_hitec=(g*beta_hitec*(T_phitec(m)-T_wall_hitec)*H_p^3)/nu_hitec^2;
    Ra_hitec=Gr_hitec*Pr_hitec;
    sci_hitec=(1+(.492/Pr_hitec)^(9/16))^(-16/9);
    if (Ra_hitec<10^9)
        Nu_hitec=.68+.67*(Ra_hitec.*sci_hitec).^(1/4);
    else
        Nu_hitec=.15*(Ra_hitec*sci_hitec)^(1/3);
    end
    h_nw_hitec=Nu_hitec*k_hitec/H_p;
    A_ht=2*H_p*(L_p+W_p);
    Q_nw_hitec=(T_phitec(m)-T_wall_hitec)/...
        ..(L_w/k_w/A_ht+1/h_nw_hitec/A_ht); %must include conduction stuff

    %nat conv: pool to air
    L_c=L_p*W_p/(2*L_p+2*W_p);
    Gr_hitec=(g*beta_airhitec*(T_phitec(m)-TinfAir)*L_c^3)/nu_hitec^2;
    Ra_hitec=Gr_hitec*pr_air_hitec;
    if (Ra_hitec<10^7)
        Nu_hitec=.54*Ra_hitec^(1/4);
    else
        Nu_hitec=.15*Ra_hitec^(1/3);
    end
    h_na_hitec=Nu_hitec*k_air_hitec/L_c;
    Q_na_hitec=h_na_hitec*(L_p*W_p)*(T_phitec(m)-TinfAir);

    % radiation from top
    Q_ra_hitec=sigma*emiss_hitec*(((T_phitec(m)+273)^4)...
        -((TinfAir+273)^4))*W_p*L_p;
```

```
    mhitec=rho_hitec*V_p;
    % time change

    dt_hitec=mhitec*cp_hitec*dT/(inflow...
        -(Q_nw_hitec+Q_na_hitec+Q_ra_hitec));
    t_hitec(m+1)=t_hitec(m)+dt_hitec;

end
thour_hitec=t_hitec/3600;

time_to_boil_hitec=thour_hitec(length(thour_hitec)) %display result
max_T_Hitec=max(thour_hitec)% display result

%% end of program
```

Appendix B: SCALE model

```
=csas25 parm=(nitawl)
Solder
44groupndf5
read composition
 h2o 1 1 293 end
 uo2 2 1 500 end
 zirc4 3 1 500 end
 al 4 0.6 500 end
 cadmium 4 0.4 500 end
end composition
read param gen=203 npg=1000 nsk=3 end param
read geometry
unit 1
com='fuel'
cylinder 2 1 .4095 426.7 0
unit 2
com='fuel clad'
cylinder 3 1 .425 426.7 0
hole 1 0 0 0
unit 11
com='solder'
cylinder 4 1 0.4265 426.7 0
hole 2 0 0 0
unit 3
com='water block'
cuboid 1 1 .627 -.627 .627 -.627 5000 -1
hole 11 0 0 0
unit 4
com='par water'
cuboid 1 1 20.691 -.627 -.627 -1.254 5000 -1
unit 9
com='vert water'
cuboid 1 1 -.627 -1.254 20.691 -.627 5000 -1
unit 8
com='void'
cuboid 1 1 -.627 -1.254 -.627 -1.254 5000 -1
unit 5
com='bundle'
 array 1 1
end geometry
READ ARRAY
ARA=1 NUX=17 NUY=17 FILL F3 END FILL
ARA=2 NUX=7 NUY=8 FILL 8 4 8 4 8 4 8 9 5 9 5 9 5 9 8 4 8 4 8 4 8 2Q14 8 4 8 4 8 4 8 END FILL
END ARRAY
end data
end
```